Available online at www.sciencedirect.com
SCIENCE DIRECT®
Journal of Hydrology 314 (2005) 212–234
Journal of Hydrology
www.elsevier.com/locate/jhydrol

Simulation of integrated surface-water/ground-water flow and salinity for a coastal wetland and adjacent estuary

Christian Langevin*, Eric Swain[1], Melinda Wolfert[2]

US Geological Survey, 9100 NW 36th Street, Suite 107, Miami, FL 33178, USA

Received 30 November 2004; revised 17 March 2005; accepted 1 April 2005

Abstract

The SWIFT2D surface-water flow and transport code, which solves the St Venant equations in two dimensions, was coupled with the SEAWAT variable-density ground-water code to represent hydrologic processes in coastal wetlands and adjacent estuaries. A sequentially coupled time-lagged approach was implemented, based on a variable-density form of Darcy's Law, to couple the surface and subsurface systems. The integrated code also represents the advective transport of salt mass between the surface and subsurface. The integrated code was applied to the southern Everglades of Florida to quantify flow and salinity patterns and to evaluate effects of hydrologic processes. Model results confirm several important observations about the coastal wetland: (1) the coastal embankment separating the wetland from the estuary is overtopped only during tropical storms, (2) leakage between the surface and subsurface is locally important in the wetland, but submarine ground-water discharge does not contribute large quantities of freshwater to the estuary, and (3) coastal wetland salinities increase to near seawater values during the dry season, and the wetland flushes each year with the onset of the wet season.

Keywords: Surface water; Ground water; Wetlands; Variable density; Everglades

1. Introduction

Coastal wetlands are a difficult hydrologic environment to represent with a numerical model because of the large number of contributing hydrologic processes, shallow hydraulic gradients, and variable-density flow conditions. Existing numerical modeling strategies have been developed for either the freshwater wetland system or the estuary, but simulations rarely span both domains. Recently, distributed-parameter physics-based computer codes have been developed to simulate coupled surface-water and ground-water flow for inland freshwater systems. Examples include: InHM (VanderKwaak, 1999; VanderKwaak and Loague, 2001), MIKE SHE (Graham and Refsgaard, 2001), MODHMS (HydroGeoLogic Inc., 2003; Panday and Huyakorn, 2004), and WASH123 (Yeh and Huang, 2003). To simplify surface and subsurface coupling techniques and to minimize computer

* Corresponding author. Tel.: +1 305 717 5817; fax: +1 305 717 5801.
E-mail addresses: langevin@usgs.gov (C. Langevin), edswain@usgs.gov (E. Swain), mwolfert@usgs.gov (M. Wolfert).
[1] Tel.: +1 305 717 5825.
[2] Tel.: +1 305 717 5855.

0022-1694/$ - see front matter © 2005 Elsevier B.V. All rights reserved.
doi:10.1016/j.jhydrol.2005.04.015

runtimes, many integrated models use the diffusive wave approximation to the St Venant equation to represent overland flow. The diffusive wave approximation, in which the convective and local acceleration terms are neglected, is normally a valid approximation for inland systems due to relatively high frictional resistances, small flow velocities, and shallow flow depths. Most integrated models are also based on the assumption of constant fluid density, and thus their applicability to coastal regions is questionable unless it can somehow be shown that model results are insensitive to density variations. Conversely, estuary and oceanic models typically solve the full St Venant equations because the convective and local acceleration terms are significant under tidal and wind-driven conditions. Furthermore, most estuarine and oceanic models contain options for including the effects of density on surface-water flow, and have transport capabilities to simulate salinity. Estuarine and oceanic models, however, normally assume ground-water exchanges are negligible, or that the exchanges can be represented as a simple source term (Wang et al., 2003; Brown et al., 2003). Thus, most of the existing codes are not well suited to represent both the inland and marine systems, and the coastal wetlands that separate them.

This paper describes the development and application of an integrated surface-water/ground-water flow and solute-transport code designed to simulate two-dimensional overland flow and three-dimensional fully saturated ground-water flow. The integrated code was designed specifically for the coastal wetland transition zone between inland freshwater systems and marine systems. Surface-water flow and transport are simulated using the Surface-Water Integrated Flow and Transport in Two Dimensions (SWIFT2D) two-dimensional, finite-difference hydrodynamic code originally designed for estuaries (Leendertse, 1987). The SEAWAT three-dimensional, finite-difference code is used to simulate variable-density ground-water flow (Guo and Langevin, 2002). The two models are explicitly coupled with a one-timestep lag using a variable-density form of Darcy's Law for flow exchange and non-diffusive salt flux between models. The paper first describes the governing equations for flow and transport in both systems and then presents the numerical procedure for implementing the two codes in a coupled framework. Lastly, the integrated code is applied to the southern Everglades of Florida and northeastern Florida Bay to quantify flow and salinity patterns for a 7-yr period (1996–2002) and to examine the effects of selected hydrologic processes.

2. Governing equations

The subsequent governing equations are well described in the literature, and have been selected to represent hydrologic processes in coastal wetlands and adjacent estuaries. The two-dimensional vertically averaged flow equations are used for the surface flow as a compromise that allows better horizontal resolution at the cost of vertical resolution. This is justified by the observation that in coastal wetlands, it is important to accurately represent topographic relief, because variations in ground-surface elevations are of the same order as water depths, while the shallow depths make baroclinic driving—a main cause of third-dimension flow—highly ineffectual. The equations used to couple the surface-water model with the ground-water model assume that unsaturated zones are thin to absent, and leakage to the water table can, therefore, be treated as instantaneous. This assumption may limit the approach to areas with shallow water tables and highly porous materials.

2.1. Surface-water flow and solute transport

The governing equations for a shallow surface-water system consist of conservation of mass, volume, and momentum. Leendertse and Gritton (1971) and Leendertse (1987) present the following governing equations, which were modified by Swain et al. (2004) to include aerially distributed sources and sinks, describing the (1) conservation of water volume, (2) conservation of momentum in the x-direction, (3) conservation of momentum in the y-direction, and (4) solute mass transport:

$$\frac{\partial h}{\partial t} + \frac{\partial}{\partial x}(dv_x) + \frac{\partial}{\partial y}(dv_y) + q_{sg} + q_r + q_{et} = 0 \qquad (1)$$

$$\frac{\partial v_x}{\partial t} + v_x\frac{\partial v_x}{\partial x} + v_y\frac{\partial v_x}{\partial y} - fv_y + g\frac{\partial h}{\partial x} + \frac{g}{2}\frac{d}{\rho}\frac{\partial \rho}{\partial x} + Rv_x - \frac{C_d\rho_a}{d}W^2\sin\psi - k\left(\frac{\partial^2 v_x}{\partial x^2} + \frac{\partial^2 v_x}{\partial y^2}\right) = 0 \quad (2)$$

$$\frac{\partial v_y}{\partial t} + v_x\frac{\partial v_y}{\partial x} + v_y\frac{\partial v_y}{\partial y} + fv_x + g\frac{\partial h}{\partial y} + \frac{g}{2}\frac{d}{\rho}\frac{\partial \rho}{\partial y} + Rv_y - \frac{C_d\rho_a}{d}W^2\cos\psi - k\left(\frac{\partial^2 v_y}{\partial x^2} + \frac{\partial^2 v_y}{\partial y^2}\right) = 0 \quad (3)$$

$$\frac{\partial (Cd)}{\partial t} + \frac{\partial}{\partial x}(v_x Cd) + \frac{\partial}{\partial y}(v_y Cd) - \frac{\partial}{\partial x}\left(D_x d\frac{\partial C}{\partial x}\right) - \frac{\partial}{\partial y}\left(D_y d\frac{\partial C}{\partial y}\right) - q_{sg}C_{sg}d - q_r C_r d = 0 \quad (4)$$

where h is water stage [L], d is water depth [L], v_x and v_y are vertically averaged velocities in the x- and y-directions [LT^{-1}], q_{sg} is a source/sink term representing the volumetric exchange between surface water and ground water per unit area [LT^{-1}], q_r is a rainfall source term representing the volumetric rate per unit area [LT^{-1}], q_{et} is an evapotranspiration sink term representing the volumetric rate per unit area [LT^{-1}], f is the Coriolis parameter [T^{-1}], g is gravitational acceleration [LT^{-2}], ρ is water density [ML^{-3}], R is the bottom-stress coefficient [T^{-1}], C_d is the wind-stress coefficient [L^0], ρ_a is air density [ML^{-3}], W is wind speed [LT^{-1}], ψ is the angle between wind direction and the positive y-axis [degrees], k is the horizontal momentum-exchange coefficient [L^2T^{-1}], C is solute concentration for a conservative non-reactive constituent [ML^{-3}], D_x and D_y are the dispersion coefficients in the x- and y-directions [L^2T^{-1}], C_{sg} is the leakage concentration between surface water and ground water [ML^{-3}], and C_r is the solute concentration of rainfall. In this paper, the source concentration for rainfall and the sink concentration for evapotranspiration are both assumed to be zero, because C represents salinity concentration, which is considered conservative and non-reacting. The transport equation (Eq. (4)) can easily be extended to represent reactive and decaying constituents. Fluid density is related to salinity, in practical salinity units (psu), using the following equation of state:

$$\rho = \rho_f + \frac{\partial \rho}{\partial C}C \quad (5)$$

where ρ_f is the reference fluid density (that is, the density of freshwater) [ML^{-3}], and $\partial\rho/\partial C$ is the slope of a linear relation between fluid density and salinity [L^0]. For salinities ranging between freshwater and typical seawater, $\partial\rho/\partial C$ has an approximate value of 0.7. The effect of temperature on fluid density is not considered here, although it could be important for some applications. For the Everglades application, seasonal temperature variations can be substantial, but spatial variations are assumed to have a negligible effect on flow. Simultaneous solutions to Eqs. (1)–(5) result in spatial distributions for h, C, ρ, v_x, and v_y.

2.2. Ground-water flow and solute transport

Simulation of ground-water flow in an aquifer with spatially varying fluid density requires solving the three-dimensional, coupled ground-water flow and solute-transport equations. The assumption of shallow depths (used for surface-water flow) does not apply to ground water, and a full, three-dimensional solution is required to account for vertical variations in aquifer properties and flow patterns. Guo and Langevin (2002) derive a variable-density form of the fully saturated, three-dimensional ground-water flow equation in terms of h_f, which is equivalent freshwater head [L] (Lusczynski, 1961):

$$\frac{\partial}{\partial x}\left[\rho K_{f,xx}\left(\frac{\partial h_f}{\partial x}\right)\right] + \frac{\partial}{\partial y}\left[\rho K_{f,yy}\left(\frac{\partial h_f}{\partial y}\right)\right] + \frac{\partial}{\partial z}\left[\rho K_{f,zz}\left(\frac{\partial h_f}{\partial z} + \frac{\rho - \rho_f}{\rho_f}\right)\right] - \rho_{sg}q_{sg} + \rho_f q_r + \rho_f q_{et} = \rho S_f\frac{\partial h_f}{\partial t} + \theta\frac{\partial \rho}{\partial C}\frac{\partial C}{\partial t} \quad (6)$$

where $K_{f,xx}$, $K_{f,yy}$, and $K_{f,zz}$ are equivalent freshwater hydraulic conductivities [LT^{-1}] in the x-, y-, and z-directions, ρ_{sg} is the density of the leakage fluid calculated by substituting C_{sg} into Eq. (5) [ML^{-3}], S_f is the specific storage in terms of equivalent freshwater head [L^{-1}], and θ is porosity [L^0]. The governing equation for solute transport within

a porous medium (Zheng and Wang, 1999) is written as

$$\frac{\partial}{\partial x}\left(\theta D_{xx}\frac{\partial C}{\partial x}+\theta D_{xy}\frac{\partial C}{\partial y}+\theta D_{xz}\frac{\partial C}{\partial z}\right)-\frac{\partial}{\partial x}(q_x C)+\frac{\partial}{\partial y}\left(\theta D_{yx}\frac{\partial C}{\partial x}+\theta D_{yy}\frac{\partial C}{\partial y}+\theta D_{yz}\frac{\partial C}{\partial z}\right)-\frac{\partial}{\partial y}(q_y C)+\frac{\partial}{\partial z}\left(\theta D_{zx}\frac{\partial C}{\partial x}+\theta D_{zy}\frac{\partial C}{\partial y}+\theta D_{zz}\frac{\partial C}{\partial z}\right)-\frac{\partial}{\partial z}(q_z C)-q_{sg}C_{sg}=\frac{\partial(\theta C)}{\partial t} \quad (7)$$

where q_x, q_y, and q_z are the specific discharges in the x-, y-, and z-directions [LT^{-1}]. Eqs. (6) and (7) are coupled in two ways. First, the fluid density terms in Eq. (6) are related to solute concentrations through the equation of state (Eq. (5)). Second, the solute-transport equation (Eq. (7)) contains specific discharge terms (q_x, q_y, and q_z) that result from a solution to the ground-water flow equation (Eq. (6)).

2.3. Surface-water/ground-water interactions

A variety of methods, and combinations thereof, were evaluated for calculating flow interactions between surface water and ground water, including a simple Darcy equation, modified versions of the Green–Ampt infiltration equation, and a solution to the Richard's equation. Field observations and model results confirm that unsaturated zones are rarely encountered in the Everglades coastal wetlands, but if encountered, they are thin and of short duration. Based on these observations, a simple variable-density form of Darcy's equation (Juster, 1995; Guo and Langevin, 2002) written in terms of equivalent freshwater head was programmed to calculate vertical leakage between the wetlands and aquifer. If a thin unsaturated zone develops during the simulation, leakage rates are constrained such that rates do not increase as the water table drops farther below land surface (described in the next section). The leakage flux is applied as a source/sink term in the continuity equation for surface-water flow (Eq. (1)) and as a boundary flux to the aquifer surface for the ground-water system. The difference in treatment is due to a two-dimensional surface-water model and a three-dimensional ground-water model. Vertical leakage is calculated using the following variable-density form of Darcy's Law:

$$q_{sg}=-K_{f,zz}\left(\frac{\partial h_f}{\partial_z}+\frac{\rho-\rho_f}{\rho_f}\right) \quad (8)$$

In this paper, solute mass transfer between systems is assumed to occur solely through advection. Thus, the solute mass flux is simply the product of leakage and the upstream solute concentration of the leakage fluid.

3. Numerical implementation

To solve the coupled surface-water and ground-water equations presented in the previous section, the finite-difference programs, SWIFT2D and SEAWAT, were modified to run timesteps sequentially under the control of a master program called Flow and Transport in a Linked Overland/Aquifer Density Dependent System (FTLOADDS). The SWIFT2D two-dimensional hydrodynamic flow and solute-transport code was originally developed for bays and shallow estuaries (Leendertse and Gritton,1971; Leendertse, 1987). The code has been applied to Jamaica Bay, NY (Leendertse, 1972), to Delta Works, The Netherlands (Leendertse et al., 1981), to Tampa, Florida (Goodwin, 1987, 1991), to Pamlico River Estuary, NC (Bales and Robbins, 1995), to Charlotte Harbor, FL (Goodwin, 1996) and to the Neuse River Estuary, NC (Robbins and Bales, 1995). The SWIFT2D program was later modified by Swain et al. (2004) to represent overland flow in coastal wetlands and to include the effects of spatially distributed rainfall and evapotranspiration. SWIFT2D uses a finite-difference approximation to solve the surface-water equations (Eqs. (1)–(5)). SEAWAT, a combined version of MODFLOW (McDonald and Harbaugh, 1988) and MT3DMS (Zheng and Wang, 1999), was designed to solve the three-dimensional variable-density ground-water flow and solute-transport equations (Eqs. (5)–(7)) using finite-difference methods (Guo and Bennett, 1998; Guo and Langevin, 2002; Langevin et al., 2003). Examples of SEAWAT applications include simulation of submarine ground-water discharge to a marine estuary (Langevin, 2001; 2003) and intercode comparisons (Bakker, 2003; Bakker et al., 2004).

SWIFT2D uses an alternating-direction implicit (ADI) method and a space- and time-staggered grid to solve the governing equations, such that each surface-water timestep is divided into two half timesteps-one half timestep for flow and transport in the x-direction and the other for the y-direction. In each of the two phases of the ADI method, the continuity equation and one of the components of the momentum equations are solved with local storage (and corresponding transport term of the continuity equation), local acceleration, pressure gradient, and the frictional term of the momentum equation treated implicitly. The last three terms on the left-hand side of Eq. (1) (the source and sink terms) are not included in the finite-difference solution, but are separately added to, or subtracted from, the cell volume. SEAWAT uses an implicit finite-difference approximation to solve the ground-water flow equation (Eq. (6)), and contains several alternative methods for solving the solute-transport equation (Eq. (7)), including implicit and explicit finite-difference methods with various weighting options and the method of characteristics.

The integrated code for SWIFT2D and SEAWAT requires cells that coincide and are identical in size. The integrated code was designed such that the domains of the two models need not be identical, provided that leakage fluxes can be neglected in areas where the two models do not overlap. Although not used for the Everglades application, this feature may prove useful for certain applications where the extension of the model domain is necessary in only one of the two systems.

3.1. Coupling procedure

Panday and Huyakorn (2004) discuss several options for coupling surface and subsurface models: (1) a 'fully coupled' or 'fully implicit' approach, (2) a sequentially coupled approach in which the interaction flux is applied as a boundary condition to each model, or (3) a sequentially coupled approach in which the head for one system acts as a general-head boundary for the other system. Fairbanks et al. (2001) demonstrate that the fully implicit approach, in which a single set of matrix equations is formulated for both systems, is the most robust and accurate. Reported applications with the 'fully coupled' approach have been limited to using a diffusion analogy or kinematic wave approximation for the overland flow system. The sequentially coupled approaches may be programmed to use an iterative coupling scheme, in which solutions are repeated for the same timestep until the change between subsequent interaction fluxes is less than a user-specified value, or a time-lagged approach. One advantage of the sequentially coupled approach (used here) is that many sub-timesteps can be used for the surface model before solving for a longer subsurface timestep (Fairbanks et al., 2001). This advantage is particularly useful for the Everglades application, where surface-water timesteps are constrained far more severely than ground-water timesteps because of rapid surface-water wave propagation speeds.

A sequentially coupled time-lagged approach was implemented to couple the surface-water and ground-water systems. The approach is mass conservative in that the exact leakage flux imposed on the surface-water system is also imposed on the ground-water system. For a single ground-water stress period (m), hydraulic stresses are assumed constant. First, surface-water flow is simulated for each sub-timestep (n) by applying a leakage rate calculated with the ground-water head from the end of the previous stress period and the surface-water level at the current sub-timestep. To ensure conservation of fluid mass, individual leakage quantities for each surface sub-timestep are summed according to the following equation to calculate a time-weighted average leakage rate, $\bar{q}_{sg}^{m}$, for the stress period:

$$\bar{q}_{sg}^{m} = \frac{\sum_{n=1}^{nsub} \Delta t_n q_{sg}^{m,n}}{\sum_{n=1}^{nsub} \Delta t} \tag{9}$$

where m is stress period number, nsub is the number of sub-timesteps in the stress period, and Δt is the sub-timestep length. This average leakage rate is then applied to the ground-water model as a specified-flux boundary that remains constant for the stress period.

3.2. Leakage calculation

The leakage flux is calculated in one of three ways, depending on the presence of standing surface water and the vertical position of the water table. For sub-timesteps with a dry surface-water cell, the leakage flux is set to zero. For cells with standing surface water, the leakage formulation is based on a variable-density form

of Darcy's Law, where the conductance term is calculated using the mean hydraulic conductivity between land surface and the vertical center of the top aquifer layer (Fig. 1). Thus, the leakage flow length is from land surface to the center of the top aquifer layer, where the equivalent freshwater head is calculated by SEAWAT. The formulation allows for the presence of a thin, hydraulically resistive layer at the land surface, which for the Everglades application, corresponds to the peat and marl unit overlying the Biscayne aquifer. Thus, for cells where the surface-water level, $h_{i,j,0}$, is above land surface, $Z_{i,j,0}$, and the water-table elevation, $h_{i,j,1}$, is above the bottom of the thin layer (as shown in Fig. 1), the leakage flux is calculated using the following variable-density form of Darcy's Law:

For $h_{i,j,0} > Z_{i,j,0}$ and $h_{i,j,1} \geq Z_{i,j,\mathrm{TL\_BOT}}$,

$$q_{\mathrm{sg}} = \frac{K_{\mathrm{f},i,j,1/2}}{0.5\Delta Z_{i,j,1}}\left[h_{\mathrm{f},i,j,0} - h_{\mathrm{f},i,j,1} + \frac{\rho_{i,j,1} - \rho_{\mathrm{f}}}{\rho_{\mathrm{f}}}(Z_{i,j,0} - Z_{i,j,1})\right] \tag{10}$$

where $Z_{i,j,\mathrm{TL\_BOT}}$ is the elevation of the thin layer bottom [L], $K_{\mathrm{f},i,j,1/2}$ is the thickness-weighted harmonic mean average of equivalent freshwater hydraulic conductivity between 1 and surface and the center of aquifer layer 1 [LT^{-1}], $\Delta Z_{i,j,1}$ is the layer 1 cell thickness, $\mathrm{K_{f,i,j,1/2}}$ is the equivalent freshwater head [L]

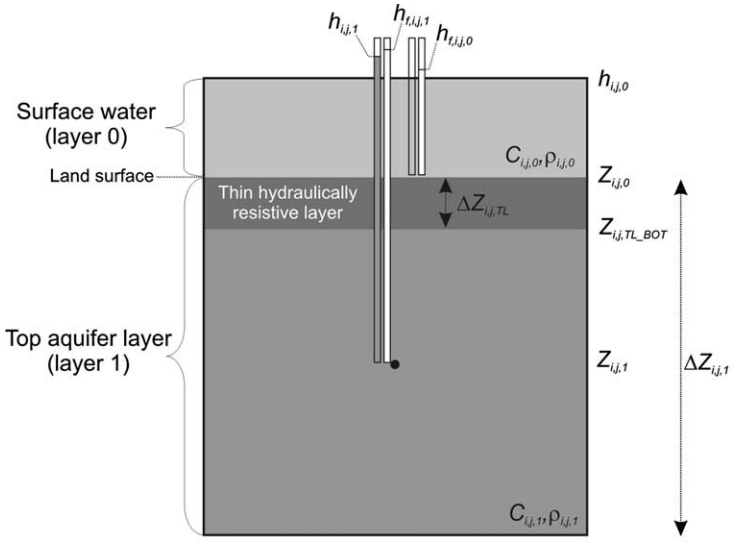

EXPLANATION

$h_{i,j,1}$ is the head in a piezometer open at the center of aquifer layer 1
$h_{f,i,j,1}$ is the equivalent freshwater head in a piezometer open at the center of aquifer layer 1
$h_{i,j,0}$ is the elevation of the water surface
$h_{f,i,j,0}$ is the equivalent freshwater head in a piezometer open at land surface
$C_{i,j,0}$ is the solute concentration of the surface water
$\rho_{i,j,0}$ is the density of the surface water
$C_{i,j,1}$ is the solute concentration of the ground water in aquifer layer 1
$\rho_{i,j,1}$ is the density of the ground water in aquifer layer 1
$Z_{i,j,0}$ is the elevation of land surface
Z_{i,j,TL_BOT} is the elevation at the base of the thin layer
$\Delta Z_{i,j,TL}$ is the thickness of the thin layer
$Z_{i,j,1}$ is the center elevation of aquifer layer 1
$\Delta Z_{i,j,1}$ is the thickness of aquifer layer 1

Fig. 1. Surface-water cell and uppermost aquifer cell. Piezometers are used to demonstrate the concept of equivalent freshwater head and the reference elevations for calculating equivalent freshwater head.

of the surface water (layer 0) evaluated at land surface, is the equivalent freshwater head [L] at the vertical center of layer 1, $\rho_{i,j,1}$ is the ground-water fluid density [ML^{-3}], and $Z_{i,j,1}$ is the center elevation [L] for layer 1.

Although rare for the Everglades application, a thin unsaturated zone can develop if the surface-water layer is rapidly flooded while the water table remains below the bottom of the thin hydraulically resistive layer. If these conditions occur in the model, Eq. (10) is no longer valid, and it is assumed that the entire head loss between land surface and the center of the cell occurs across the thin layer. With this assumption and the assumption that the pressure at the bottom of the thin layer is atmospheric, the following equation is used to approximate the flux through the thin unsaturated zone:

For $h_{i,j,0} > Z_{i,j,0}$ and $h_{i,j,1} < Z_{i,j,\mathrm{TL\_BOT}}$,

$$q_{\mathrm{sg}} = -\frac{L_{\mathrm{f,i,j,TL}}}{\Delta Z_{\mathrm{i,j,TL}}}\left[h_{\mathrm{f,i,j,0}} - Z_{\mathrm{i,j,TL\_BOT}} + \frac{\rho_{\mathrm{i,j,0}} - \rho_{\mathrm{f}}}{\rho_{\mathrm{f}}}\Delta Z_{\mathrm{i,j,TL}}\right] \tag{11}$$

where $K_{\mathrm{f},i,j,\mathrm{TL}}$ is the vertical equivalent freshwater hydraulic conductivity of the thin layer [LT^{-1}], $\Delta Z_{i,j,\mathrm{TL}}$ is the thickness of the thin layer [L], and $\rho_{i,j,0}$ is the density of the surface water [ML^{-3}]. This approximation for the flux through the unsaturated zone is based on the approach used by MODFLOW (McDonald and Harbaugh, 1988) and SEAWAT (Guo and Langevin, 2002) for the River package. A more sophisticated approach, such as one based on a modified Green–Ampt formulation may be required if future applications result in ponded surface water overlying a relatively thick unsaturated zone. A limitation with the sequentially coupled time-lagged approach used here is that ground-water stress periods must be set short enough to adequately capture the temporal scales of interest.

3.3. Surface/subsurface solute exchange

A mass-conservative approach was designed to allow advective transport between the wetland and underlying aquifer. Calculation of the advective mass flux is straightforward for most stress periods in which the advective flux is either up or down for the entire period. If leakage is downward, the advective mass flux is the product of the leakage rate and the surface-water solute concentration. Likewise, for upward leakage, the advective mass flux is the product of the leakage rate and the ground-water solute concentration.

Concentration changes that result from advective transport between the wetland and aquifer are calculated for each sub-timestep in SWIFT2D. To account for advective leakage transport in the ground-water model, the total solute mass added to, and subtracted from, the surface-water cell is summed in SWIFT2D for each stress period. This total mass transferred is then divided by the total leakage volume for that stress period to calculate an effective leakage concentration. Thus, the volumetric leakage rate applied to SEAWAT has an associated effective concentration that results in the conservation of mass between the two systems. If multiple reversals of leakage direction occur during a single stress period, the effective concentration can be very small or even negative. If a highly saline ground-water system is overlain by a fresh surface-water system and leakage reverses direction multiple times, then the net salt transfer will be upward even if the net leakage is downward. In this case, the effective concentration will be negative indicating that the net salt flux is in the opposite direction of the net volume flux.

3.4. Spatially distributed rainfall and evapotranspiration

The original SWIFT2D program was modified to include spatially distributed rainfall and evapotranspiration (Swain et al., 2004). For conditions with standing surface water, rainfall is applied to the surface-water layer with a solute concentration of zero. If a surface-water cell is dry, the rainfall volume is applied directly and instantaneously to the water table in layer 1 of the ground-water model. The same approach is used to determine where the evapotranspiration flux is applied. In the current Everglades application, however, the evapotranspiration flux is calculated by the model during the simulation using a modified Priestly–Taylor approximation to the physics-based Penman–Monteith model as described by German (2000a,b) and Swain et al. (2004). Evapotranspiration rates are calculated as a function of solar radiation and water depth. Two sets of coefficients were estimated through linear regression and used in

the Priestly-Taylor approximation. One set was calculated for conditions with standing water; the other was calculated for dry surface-water conditions when the water table was below land surface. For conditions with standing water, the entire evapotranspiration flux is withdrawn from surface water, rather than withdrawing evaporation from surface water and transpiration from ground water. The dependency on water depth is unusual, but appears to be related to sheltering by vegetation and submergence of vegetation (German, 1999).

3.5. Rewetting

In the present integrated code, surface-water and ground-water cells are allowed to dry and rewet. The original versions of SWIFT2D and SEAWAT both have options for cells to rewet from the four surrounding nodes, and in the case of SEAWAT, from an underlying node. Rewetting in SEAWAT is a simple extension of the procedure implemented in MODFLOW (McDonald et al., 1992). In the integrated program, a modification was made to SWIFT2D to allow surface-water cells to rewet from the underlying ground-water cell if the water table rises above land surface. If a surface-water cell is dry, then SWIFT2D compares surrounding stages and height of the water table with land-surface elevation. This comparison is performed for a sub-timestep interval provided by the user. If a surrounding stage or water-table elevation is above land surface, the cell is reactivated and included in the computational domain for the subsequent sub-timestep. SWIFT2D also conserves solute mass during drying and rewetting by storing any remaining solute mass during dry periods and adding that mass upon rewetting.

4. Application of integrated model to the southern Florida Everglades

The integrated model was applied to a 900-km^2 area of the southern Everglades and northeastern Florida Bay (Fig. 2) to evaluate the dominant hydrologic processes, including surface-water and ground-water interactions, and to evaluate the mechanisms of freshwater delivery to northeastern Florida Bay. Detailed descriptions of the modeling project are given in Langevin et al. (2004) and Swain et al. (2004). The southern Everglades consist of two main hydrologic features called Shark and Taylor Sloughs. Both sloughs are contained within shallow topographic depressions, are slow flowing, and are capable of transmitting substantial water volumes due to their expansive cross-sectional widths. The present study is focused on Taylor Slough, which is the smaller of two main sloughs in southern Florida. Rainfall is a dominant source of freshwater for the study area, which receives an average of about 140 cm yr^{-1}. About 75% of the rainfall occurs during the five wet-season months from June to October (Langevin, 2001). Inflows also occur by means of a water-management canal system that controls water levels in southern Florida to prevent flooding. On the west side of the study area, culverts beneath the Main Park Road allow surface water to exchange with the wetlands to the west, but flow measurements indicate the exchanges are minimal (Tillis, 2001; Stewart et al., 2002).

A principal hydrologic feature in the study area is the Buttonwood Embankment—a nearly continuous ridge along the Florida Bay coastline. This ridge is observed to be about 0.3 m higher than the surrounding marsh, and was formed either by the buildup of organic detritus from the stands of mangrove forest or by sediment deposition from Florida Bay during periodic hurricanes and tropical storms (Holmes et al., 2000). The ridge itself forms a partial low-crowned barrier and obstructs direct overland flow from the coastal wetlands into northeastern Florida Bay at most times. Hydraulic connection between the coastal wetlands and northeastern Florida Bay occurs through coastal creeks that have incised the Buttonwood Embankment and possibly through the underlying sediments. Overtopping is infrequent and is typically caused by northward moving storms or hurricanes that force brackish Florida Bay water over the embankment and into the coastal wetlands (Hittle, 2000).

Field studies of surface-water and ground-water interactions within the Taylor Slough area are reported by Harvey et al. (2000a,b) and Price (2001). Using a chloride dilution method, Harvey et al. (2000a) indicated that: (1) upward ground-water flow in November 1997 may have been as large as 3 cm d^{-1} in the area near NP67 and TSH (Fig. 2), (2) the high water levels on the northwestern side of Old Ingraham

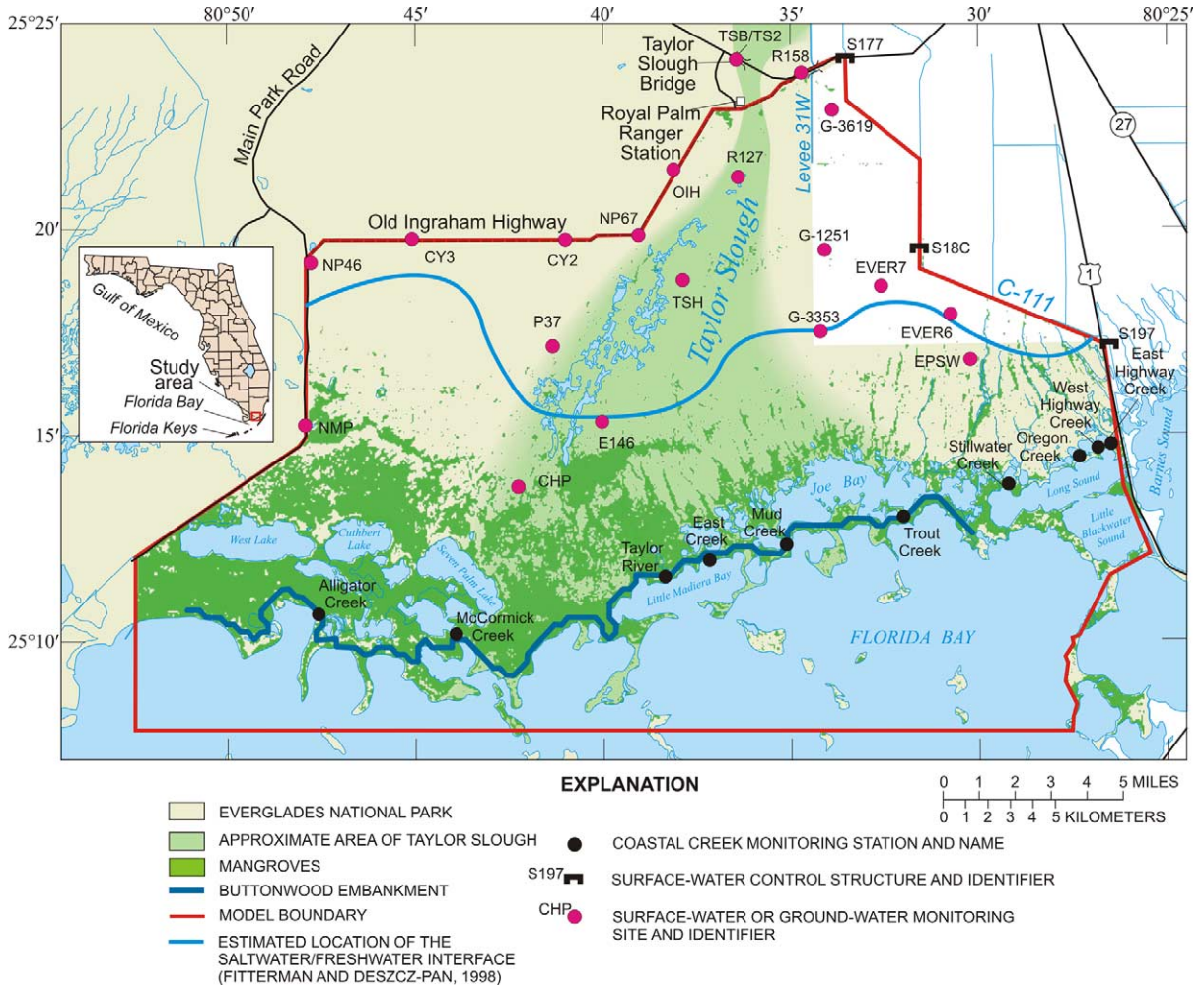

Fig. 2. Study area showing location of Taylor Slough, Florida Bay, monitoring stations, and domain of numerical model.

Highway are probably driving ground-water flow into the western part of Taylor Slough, and (3) upward ground-water flow within the slough itself is about 0.06 cm d^{-1} for the period between September 1997 and September 1999. Using a variety of geochemical tracers, Price (2001) estimated leakage rates that ranged over four orders of magnitude.

Salinity patterns in northeastern Florida Bay are highly influenced by freshwater discharges from the coastal wetlands (Hittle, 2000; Nuttle et al., 2000). Flows from coastal creeks appear to be the dominant source of freshwater for northeastern Florida Bay, although an unresolved question has been the importance of Buttonwood Embankment overtopping and terrestrially derived ground water discharge. Substantial freshwater inputs into Florida Bay from shallow ground water seem unlikely because recent helicopter electromagnetic surveys revealed that shallow saline ground water extends at least 7 km inland (Fig. 2; Fitterman and Deszcz-Pan, 1998).

4.1. Model design

The finite-difference model grid used for the Everglades application consists of 98 east–west rows and 148 north–south columns. Model cells are square and measure 305 m (1000 feet) per side. The area of

the model that corresponds to the coastal wetlands (the active model area north of the Buttonwood Embankment) is about 6.2×10^8 m^2. Florida Bay comprises about 2.8×10^8 m^2 of the model area. Land-surface elevations were calculated by interpolating values from a helicopter global positioning system (GPS) survey with 400-m spacing between measurements (Desmond, 2003). Data from National Oceanic and Atmospheric Administration nautical charts and from Hansen and Dewitt (2000) were used to assign bathymetry for Florida Bay and its subembayments. The Buttonwood Embankment was included in the model using the weir barrier feature in SWIFT2D with a specified sill height of 0.3 m above land surface. Flow over the embankment is calculated using either the submerged or free weir equation depending on the downstream condition. The three-dimensional ground-water model was designed using as many model layers as possible to achieve adequate vertical resolution while maintaining acceptable computer simulation times. Thus, the aquifer was evenly divided into 10 ground-water model layers. The top layer extends from land surface to an elevation of 3.2 m below NAVD 88 (North American Vertical Datum of 1988). The remaining layers are uniform in volume and have a constant thickness of 3.2 m. The ground-water model extends from land surface to the base of the Biscayne aquifer, as defined by Fish and Stewart (1991) and revised by Fitterman et al. (1999). The lower part of the surficial aquifer system, as described by Jarosewich and Wagner (1985) and Fish and Stewart (1991), is not included in the model. This approach treats the base of the Biscayne aquifer as a no-flow boundary—an approach commonly used in southern Florida (Merritt, 1996a,b; Swain et al., 1996; Langevin, 2001) and justified by the sharp contrast in permeabilities.

Boundary conditions for the surface-water model were specified for the model perimeter based on the presence of roads, canals, culverts, islands, and an estimated sufficient offshore distance from the southern Florida coastline. A combination of specified flux and specified water level were assigned for the inland surface-water model boundaries. Surface-water fluxes into the coastal wetland were specified using measured discharges at various locations within the water-management system. Water-level boundaries were specified using recorded stage measurements. Offshore, no-flow conditions were specified along linear island segments, whereas interpolated water levels were specified for open-water boundaries. Two different types of boundaries were used for the ground-water model. North of the Florida Bay coastline, general-head boundaries were applied to each layer of the ground-water model based on interpolated head values from nearby surface-water and ground-water monitoring sites for each day of the simulation period. Salinity values assigned to the general-head boundaries in all layers were estimated from the airborne geophysical survey (Fitterman and Deszcz-Pan, 1998). South of the Florida Bay coastline, a no-flow boundary was imposed on the ground-water model. The no-flow condition was assigned based on the assumption that the boundary is far south (about 1–10 km) of the area where ground-water discharge might occur. Simulated leakage maps confirmed this assumption. Additional details on the boundary types are given in Langevin et al. (2004) and Swain et al. (2004).

Rainfall and evapotranspiration are the primary sources and sinks within the model domain. Rainfall data were spatially interpolated (kriged) for each model cell and time interpolated for each surface-water sub-timestep using measured rainfall values at approximately 14 stations located within or near the model domain. Evapotranspiration was included in the model using a modified form of the Priestly Taylor approximation as previously described.

The surface-water simulation is controlled by spatially varying parameters that represent relevant processes. This includes defining the frictional resistance to flow, wind friction factor and sheltering coefficient, and dispersion coefficient. The frictional resistance to flow is expressed with Manning's coefficients. Because of the importance of this term, field and laboratory research was performed to determine the effective frictional resistance to water flow through differing Everglades vegetation types (Lee et al., 1999, 2000). Results of these studies indicate high Manning's n values and relatively small variations between vegetation types. Assigned values of Manning's n vary spatially in the model based on a remotely sensed vegetation map and range from 0.38 to 0.46 s m$^{-1/3}$ (Swain et al., 2004). Open-water areas are assigned a nominal value of 0.02 s m$^{-1/3}$. Frictional resistance values for the coastal creeks

were determined by calibration and from field measurements at the mouth of Taylor River (Fig. 2) and another station (not shown) about 3 km inland from the mouth. The calibrated values of Manning's n for the coastal creeks ranged from 0.058 to 0.152 s $m^{-1/3}$. The coefficient for the wind-friction term that related the wind velocity squared to the rate of momentum change in the water flow has a specified value of approximately 1.2×10^{-3} for winds less than 36 m s^{-1} (Large and Pond, 1981). This coefficient is uniform for the entire study area. A wind-sheltering term also is applied to account for the effects of emergent vegetation. Estimated values for this wind-sheltering term range from 0.1 to 0.5 (Reid and Whitaker, 1976); a value of 0.33 is used in the model. Jenter and Duff (1999) suggest that the values estimated by Reid and Whitaker (1976) are reasonable for the Everglades coastal wetlands. The magnitude of the dispersion coefficient for surface water is scale dependent, increasing with the size of the water body. The effective dispersion coefficient is on the order of 1–10 m^2 s^{-1} in open channels, and two orders of magnitude greater in estuaries (Fischer et al., 1979). In the application of the dispersion coefficient in a numerical model, the length scale of importance is the cell size. Therefore, the dispersion coefficient was calibrated by matching salinity values at the coastal creek measurement stations.

Application of Darcy's Law to calculate leakage rates (Eq. (9)) required an assignment of aquifer properties to the upper half of layer 1 of the ground-water model. The current program reads the thickness and vertical hydraulic conductivity of the thin layer and the vertical hydraulic conductivity of the part of the aquifer between the base of the thin layer and the vertical center of model layer 1. Values for these parameters were assigned based on studies by Harvey et al. (2000a,b), which measured hydraulic properties of the thin peat layer using standard slug testing techniques. For Florida Bay, leakage coefficients were assigned based on mapped bottom types (Prager and Halley, 1997). For hard-bottom areas such as Joe Bay, a vertical aquifer hydraulic conductivity value of 0.75 m d^{-1} was used. All other bottom types in Florida Bay were assumed to have a 1 m thick sediment layer with a vertical hydraulic conductivity value of 0.1 m d^{-1}. The remaining part of the Biscayne aquifer was assumed to be isotropic and homogeneous with vertical and horizontal hydraulic conductivity values of 0.75 and 5000 m d^{-1}, respectively. These values, which were determined through calibration, compare closely with values used in other numerical models of the area (Merritt, 1996a,b; Swain et al., 1996; Langevin, 2001).

Limited data exist on the dispersive properties of the Biscayne aquifer. Merritt (1996b) was able to estimate dispersive parameters based on the calibration of a transport model to simulate a chloride plume that resulted from a flowing artesian well open to the brackish Floridan aquifer. For the present simulation, however, hydrodynamic dispersion within the ground-water model was not active during the integrated simulations. Preliminary ground-water simulations indicated that the position of the freshwater/saltwater interface in the Biscayne aquifer was adequately simulated without explicitly representing hydrodynamic dispersion. Future applications of the integrated model would benefit from a more rigorous representation of ground-water hydrodynamic dispersion.

4.2. Model calibration

Computer runtimes in excess of 30 h (on a Pentium IV processor running at 1.7 GHz) for the 7-yr simulation period prohibited use of formalized parameter estimation techniques. Instead, calibration was achieved by judicious adjustment of the input parameters that seemed to have the largest uncertainty range and the largest effect on simulation results. Calibration statistics for coastal creek discharges, wetland stages, and creek salinities are reported in Table 1. In addition to the model results given in Table 1, other model results were also compared with field data. For example, the simulated aquifer salinities were carefully evaluated to ensure the model adequately matched the results from an airborne electromagnetic survey (Fitterman and Deszcz-Pan, 1998). Additional descriptions of the model calibration procedure, including detailed comparisons of measured and simulated stages, heads, salinities, and discharges are given in Langevin et al. (2004) and Swain et al. (2004).

Table 1
Calibration statistics for daily average coastal creek discharges, surface-water stage or ground-water head, and coastal creek salinities

Station	ME	MAE	RMSE	Count
Discharge ($m^3 s^{-1}$)				
McCormick	0.20	1.56	2.04	2510
Mud	0.39	1.86	3.86	2530
Trout	−1.78	5.01	7.06	2526
Taylor River	−0.23	1.21	2.90	2554
West Highway	−0.30	1.10	1.65	2479
Stage/Head (m)				
NMP	0.02	0.02	0.02	2290
CY3	−0.07	0.07	0.07	2275
NP46	0.00	0.06	0.09	2475
NP67	0.01	0.06	0.08	2493
CY2	−0.03	0.04	0.05	2222
TSH	0.00	0.06	0.08	2527
E146	0.05	0.06	0.09	2477
CHP	−0.02	0.06	0.08	2473
EPSW	0.08	0.09	0.10	2461
EVER 6	−0.04	0.06	0.07	2394
EVER 7	−0.04	0.05	0.07	2444
R127	0.02	0.07	0.10	2494
P37	0.00	0.05	0.07	2465
G-3619	−0.04	0.09	0.12	2438
G-3353	0.14	0.15	0.17	2451
G-1251	0.04	0.08	0.10	2034
Salinity (psu)				
McCormick	2.76	7.14	9.43	2508
Mud	2.10	3.95	5.08	2421
Trout	2.33	4.86	6.45	2529
Taylor River	4.95	6.35	7.70	2515
West Highway	−1.43	4.60	5.57	2512

Mean errors were calculated by subtracting measured values from simulated values. Station locations are in Fig. 2. [ME, mean error; MAE, mean absolute error; RMSE, root mean square error; Count, number of data points used to calculate statistics; $m^3 s^{-1}$, cubic meters per second; psu, practical salinity units].

4.3. Model results

A water budget was prepared from model results for the coastal wetland part of the model domain, north of the Florida Bay coastline (Fig. 3). The water budget is for surface water and does not include lateral ground-water flows or evapotranspiration directly from the water table, which is about 45 cm. Water budget components are given as annual average values for the 7-yr simulation period (Fig. 3). Coastal creek discharges, and other discharge values, were divided by the wetland area (6.2×10^8 m^2) to give length units that can be compared directly with rainfall and evapotranspiration. The average annual water budget for the coastal wetland shows the relative magnitude of the different hydrologic processes and the spatial distribution of surface-water inflows and outflows (Fig. 3). Of the average annual rainfall total (138 cm), 83 cm is lost to surface-water evaporation and 38 cm is lost to direct infiltration to the water table as a result of dry surface-water cells. The remaining 17 cm combines with boundary inflows from Taylor Slough Bridge (13.7 cm), L-31W (4.3 cm), and C-111 (25.0 cm) and discharges into Florida Bay through the coastal creeks.

Discharge of fresh or brackish water from the Florida mainland into northeastern Florida Bay can occur in three ways: (1) discharge from coastal creeks, (2) overtopping of the Buttonwood Embankment, and (3) submarine ground-water discharge. Of these three discharge mechanisms, coastal creek discharge is the only one that has been directly measured in the field, and continuous measurements for 1996–2002 are available at five of the 10 coastal creeks in the area. The distribution of coastal creek discharge to Florida Bay was evaluated by using measured discharge volumes for the five creeks with continuous data for the 7-yr simulation period and simulated discharge volumes for the remaining five creeks. For the 7-yr simulation period, Trout Creek contributed nearly half (47%) of the discharge to Florida Bay. West Highway, East, Taylor River, and Mud Creeks were the next largest contributors with 12, 10, 8 and 7% of the total discharge, respectively. The five remaining creeks (Oregon, Alligator, Stillwater, McCormick, and East Highway) each contributed 5% or less of the total discharge.

The coastal creeks show distinct seasonal patterns in discharge to Florida Bay. For example, at the monthly timescale, simulated and measured discharges at Trout Creek peak during the wet season and reverse directions during most dry seasons (Fig. 4). Discharge volumes begin to increase with the onset of the wet season, which typically occurs between May and June. By September or October of each year, discharge volumes reach their annual peaks and then begin to decline as the dry season approaches in November. During some dry season months, discharge rates are negative, which indicate

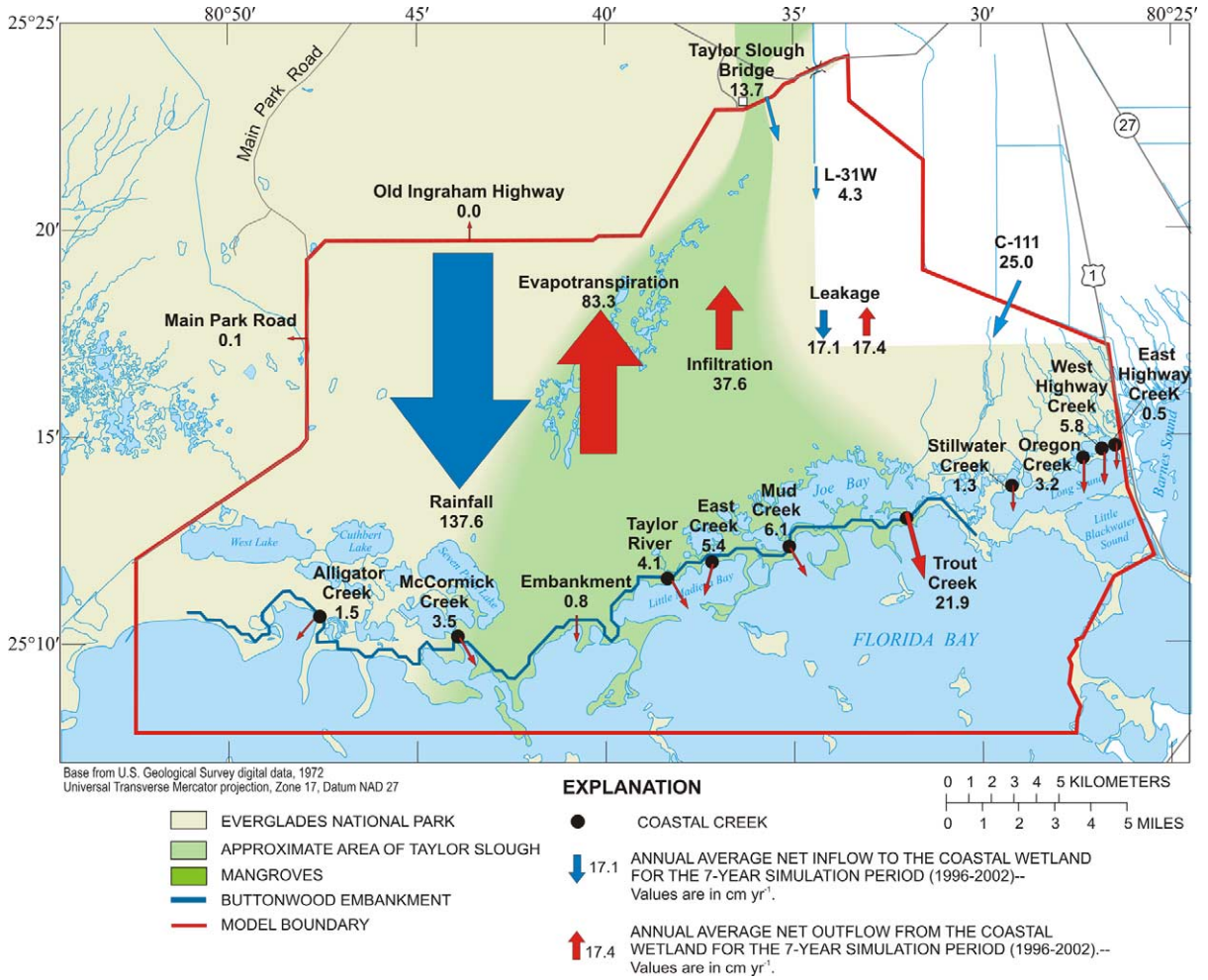

Fig. 3. Annual average surface-water budget for the surface-water system of the coastal wetland for the 7-yr simulation period (1996–2002). All values are reported in length units (cm) for direct comparison with rainfall and evapotranspiration. Boundary and coastal creek inflows or outflows are given as net values. Although not shown on this figure, an additional 45 cm of evapotranspiration is withdrawn from the water table. The discrepancy between total inflow and outflow is due to changes in storage and numerical error.

northward flow from Florida Bay into the coastal wetlands. These negative discharge rates, which are reproduced by the model, are primarily caused by sustained periods of southerly winds that push brackish Florida Bay water inland. The ability of the model to match these negative discharge values proved to be critical in accurately representing salinity values in the coastal wetlands. For the entire 7-yr period, the average monthly discharge volume calculated with measured data is 1.7×10^7 m^3 (Fig. 4). The average monthly discharge volume calculated using simulated data is 1.2×10^7 m^3, about 27% too low. Using the measured and simulated records in Fig. 4, the R^2 value is 0.77. The discrepancy appears to be caused by failure of the model to capture peak flows during the wet season. A possible explanation is that one or more of the inflows represented by the model is based on inaccurate field data. The model is highly sensitive to rainfall, and small errors in rainfall values, when applied to a large area, can lead to substantial errors in creek discharge. At shorter timescales, negative discharge values occur frequently throughout the year. Fig. 5 shows daily discharge volumes at Trout Creek for

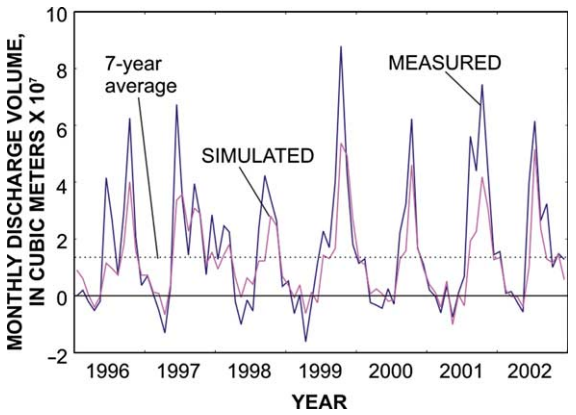

Fig. 4. Measured and simulated monthly discharge at Trout Creek from 1996 to 2002. Dashed line represents the 7-yr average daily discharge volume calculated from field measurements.

1999. Again, the model seems to represent the range in discharge volumes, capturing both the high and low values. The model does, however, fail to represent some of the higher peaks, which results in a 20% underestimation of average annual discharge volume at Trout Creek for 1999. Using daily average flows, the R^2 value for measured and simulated discharges at Trout Creek is 0.78.

Spectral analysis was performed on discharge data at Trout Creek to determine if the dominant frequencies observed in the field measurements are represented by the model. Fig. 6 shows an amplitude spectrum of measured and simulated discharge for the 7-yr dataset at Trout Creek. Four distinct spikes in the spectrum are shown at frequencies of 0.93, 1.00, 1.93, and 2.00 cycles per day in both the measured and simulated discharges. The spike at 0.93 corresponds to the O1 tidal component, which has a period of 25.8 h. At this frequency, the amplitude spectrum values for the measured and simulated discharges are 0.209 and 0.208 $m^3\,d^{-1}$, respectively. The 1.00 and 2.00 cycles per day frequencies correspond to periods of 24 and 12 h, respectively, and are caused by temporal variations in wind, and possibly the S1 and S2 solar tides. Dominant spikes at the 1.00 and 2.00 frequencies are also seen in the spectrum of wind velocity (not shown) collected at the Joe Bay weather station. At the 1.00 cycle per day frequency, the amplitude spectrum values for the measured and simulated discharge are 0.529 and 0.763 $m^3\,d^{-1}$, respectively. At the 2.00 cycle per day frequency, the amplitude spectrum values for the measured and simulated discharge are 0.394 and 0.428 $m^3\,d^{-1}$, respectively. The spike at the 1.93 frequency corresponds to the M2 lunar tide. At this frequency, the simulated amplitude spectrum (0.199 $m^3\,d^{-1}$) is less than half of the measured amplitude spectrum (0.512 $m^3\,d^{-1}$). A harmonic analysis of Trout Creek stage indicates that the M2 amplitude is 0.38 cm, which is only slightly larger than the precision of the stage recorder (0.30 cm). Thus, a possible explanation for the discrepancy between the simulated and measured amplitude spectrum at the M2 frequency is that the boundary stages in the model are not recorded with enough precision to reproduce the complete M2 signal.

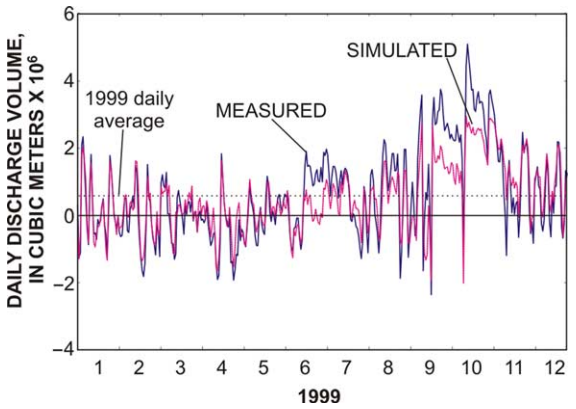

Fig. 5. Measured and simulated average daily discharge at Trout Creek for 1999.

Buttonwood Embankment overtopping is another mechanism that discharges freshwater from the coastal wetlands into Florida Bay. Due to the remote location and expansive length of the embankment, however, overtopping discharge volumes have never been measured. Elevations of the embankment crest are not available, except at the coastal creeks where estimates can be made based on the height of the embankment above the water surface. In the model grid, the embankment height is set at 0.3 m above land surface. Simulation results indicate that embankment overtopping is infrequent, but can occur in both directions in response to tropical storms. For example, as Hurricane Irene approached the Florida mainland in October 1999 (Knight et al., 2000), a storm surge was recorded at the Taylor River monitoring station (Fig. 7). This storm surge pushed a large volume of

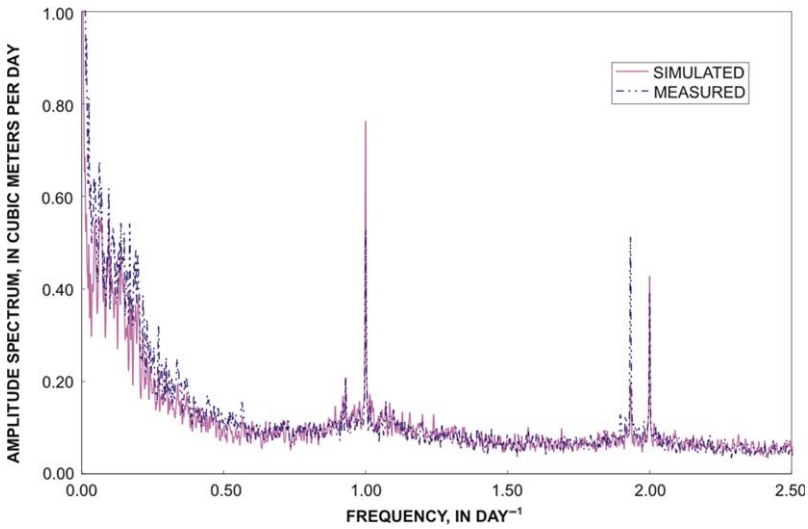

Fig. 6. Amplitude spectrum as a function of frequency calculated using 2 h measured and simulated discharges at Trout Creek for the 7-yr simulation period.

brackish water from Florida Bay over the embankment and into the coastal wetlands. After Hurricane Irene made landfall, the associated heavy rainfall reversed flow over the embankment and into Florida Bay, as indicated by the positive discharge values (Fig. 7). This was the largest overtopping event simulated by the model. For the entire 7-yr simulation period, the net overtopping discharge volume was -3.7×10^7 m^3. This suggests that although overtopping may allow for flow into the coastal wetlands, the mechanism is not a substantial source of freshwater for Florida Bay. The cumulative positive and negative overtopping discharge volumes are 7.3×10^7 m^3 and -1.1×10^8 m^3, respectively, which are relatively small compared to the cumulative creek volumes for the 7-yr simulation period (about 28×10^8 m^3 for the 10 coastal creeks). At daily, weekly, or monthly timescales, however, the overtopping volumes may be significant in terms of freshwater flows into Florida Bay, or brackish water flow into the coastal wetland.

Daily leakage rates between surface water and ground water are produced as part of the model output for each cell. These daily leakage rates were averaged

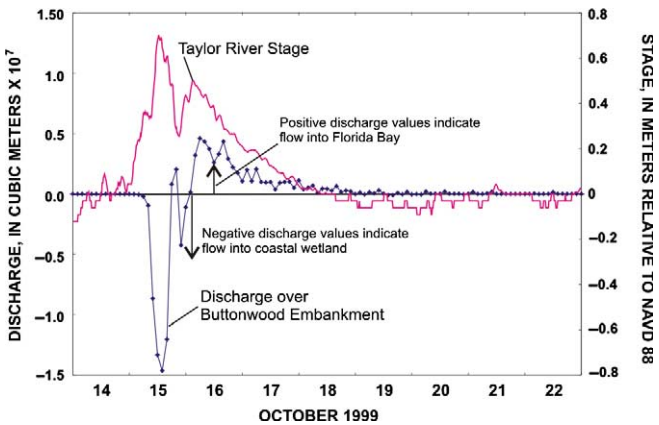

Fig. 7. Discharge over Buttonwood Embankment and stage at Taylor River during Hurricane Irene, October 1999.

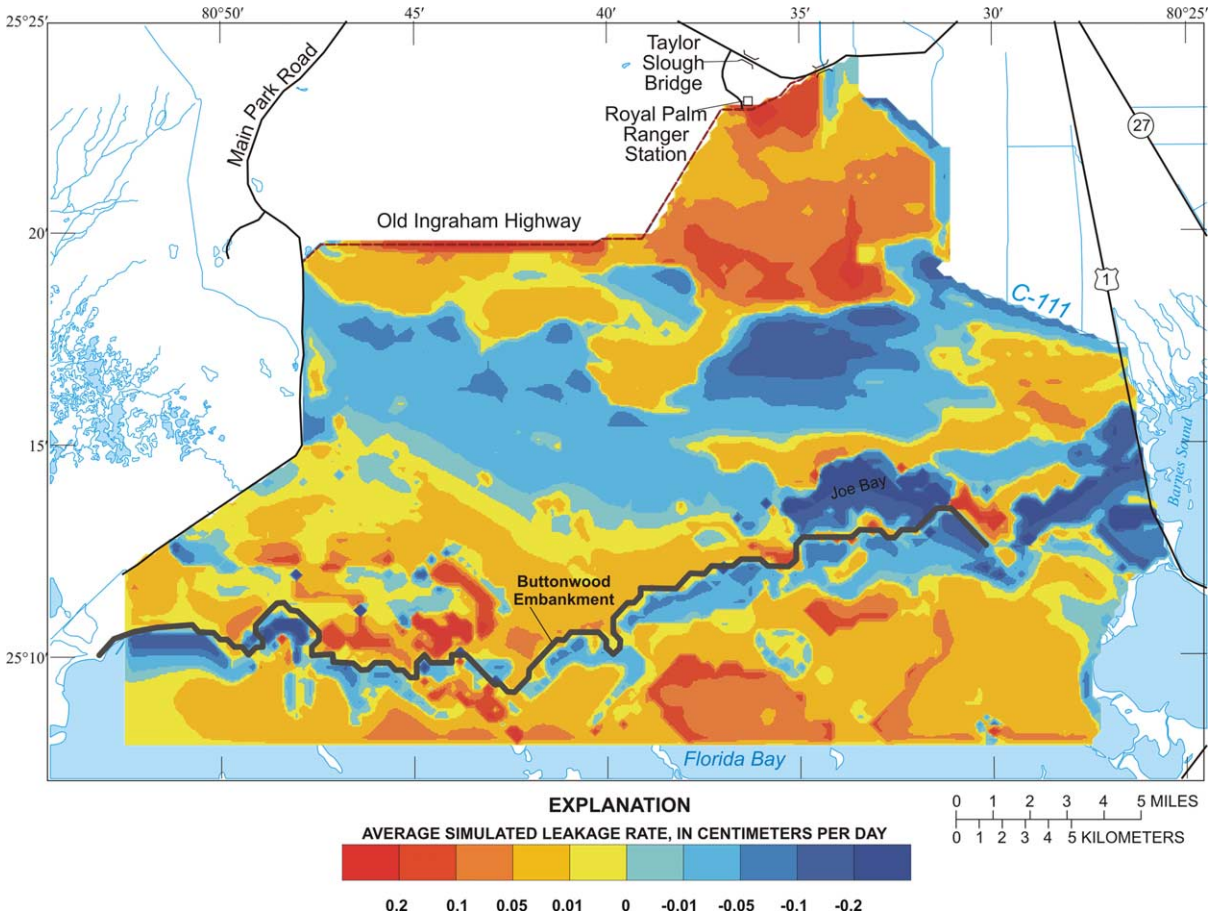

Fig. 8. Average annual leakage rates for the 7-yr simulation period. Positive values indicate downward flow into aquifer. Negative values indicate upward flow into wetland.

over the 7-yr simulation period to illustrate the spatial variability of surface-water/ground-water interaction and to determine whether ground water is discharging into Florida Bay. These leakage rates do not include recharge or evapotranspiration directly to or from the water table. The model suggests an alternating pattern of downward and upward leakage from north to south (Fig. 8). Within the wetland portion of the model domain, downward leakage rates (shown as positive values) correlate with topographically high areas. For example, in the northern part of the model, average leakage rates exceed $0.2\,\mathrm{cm\,d^{-1}}$. A band of upward leakage with rates in some areas exceeding $0.2\,\mathrm{cm\,d^{-1}}$ appears across the central part of the model. This upward leakage band correlates with a topographically low area within the central part of the model and with the freshwater/saltwater interface in the aquifer (Fig. 2). Downward leakage rates also occur just north of the Buttonwood Embankment where surface-water levels tend to be higher than those in Florida Bay. These model results suggest that there may be shallow ground-water flow beneath the embankment, which then discharges into Florida Bay. The source for this shallow ground-water flow system is surface water impounded by the Buttonwood Embankment. South of the Buttonwood Embankment, ground water discharges upward into the coastal embayments of Florida Bay. Average leakage rates within this zone can exceed $0.2\,\mathrm{cm\,d^{-1}}$, but most are between 0.01 and $0.1\,\mathrm{cm\,d^{-1}}$. Model results also indicate that Joe Bay (Figs. 2 and 8) may be a ground-water discharge area. Joe Bay has an

exposed limestone bottom, and thus, the absence of a thin layer of low-permeability sediments results in a relatively strong hydraulic connection between surface water and the underlying aquifer. Average leakage rates appear to be downward over most of Florida Bay (Fig. 8), with values ranging between about 0.0 and 0.2 cm d^{-1}. Downward leakage in this zone is probably the result of cyclic flow that often occurs in freshwater/saltwater interfaces within a coastal aquifer (Kohout, 1964; Langevin, 2001). Fresh ground water flowing toward an interface mixes with saline ground water. This brackish mixture then discharges into the ocean, coastal estuary, or in this case, into the brackish water wetlands.

Field data and model results indicate a strong seasonal pattern in coastal wetland salinities. A comparison between measured and simulated values of average monthly salinity at Trout Creek is shown in Fig. 9. Both clearly indicate season fluctuations in salinity at Trout Creek. Salinities reach 35 psu in May, June, or July of each year, which corresponds with the end of the dry season. The lowest salinities were recorded in August, September, or October of each year. A comparison of the average monthly measured and simulated salinities provides an R^2 value of 0.76. A comparison of daily salinities gives an R^2 value of 0.67, suggesting that the model is better at representing the longer seasonal fluctuations than the shorter timescale daily or weekly salinity fluctuations.

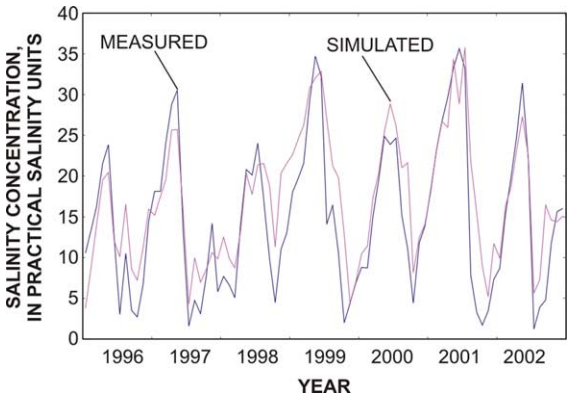

Fig. 9. Measured and simulated values of monthly average salinity at Trout Creek for the 7-yr simulation period (1996–2002).

4.4. Sensitivity analysis

Several simulations were performed to evaluate the effects of hydrologic processes unique to this particular model application, namely (1) surface-water and ground-water interactions, (2) density-dependent flow, and (3) local wind stress. These three processes are all known to be active within the study area, and thus, their effects can be evaluated by comparing simulations without these processes to the previously described integrated simulation, referred to here as the base case. A possible limitation with this approach is that the consequences for neglecting a process may be overstated if calibration of the integrated model tended to overemphasize that process.

The ground-water part of the integrated model was calibrated to heads at three monitoring wells (G-3619, G-3353, G-1251), 36 head-difference measurements, the position of the freshwater/saltwater interface, and to estimates of leakage. Further adjustments to the ground-water model did not improve simulation results, and thus the integrated model was considered calibrated within the limitations of the trial and error method. The effect of leakage on the surface-water system was evaluated by removing the ground-water model. Neglecting surface-water and ground-water interactions tends to worsen simulated discharges and salinities in most cases. Mean absolute errors (MAE) and root mean square errors (RMSE) for the simulation without leakage (Table 2) are larger (with the exception of salinity errors at McCormick Creek and Taylor River) than errors for the base case (Table 1). The average increases in MAE and RMSE for coastal creek discharge as a result of neglecting leakage are 0.54 and 0.94 $m^3\ d^{-1}$, respectively. The average increases in MAE and RMSE for coastal creek salinity are 0.14 and 0.19 psu, respectively.

In the second simulation, fluid density was held constant in space and time by adjusting the equation of state (Eq. (5)) such that concentration did not affect fluid density. The resulting cumulative flow through the five measured creeks ($1.73\times10^9\ m^3$) is about 9% less than for the base case simulation ($1.91\times10^9\ m^3$) and about 24% less than the measured cumulative discharge ($2.25\times10^9\ m^3$). Also, there is 15.3% difference in cumulative discharge for the five creeks without continuous data ($4.60\times10^8\ m^3$ compared

Table 2
Calibration statistics for the surface-water simulation without leakage

Station	ME	MAE	RMSE
Discharge ($m^3 s^{-1}$)			
McCormick	0.78	2.62	4.98
Mud	0.25	2.40	4.32
Trout	−2.13	5.74	7.86
Taylor river	−0.06	1.50	3.40
West highway	−0.29	1.18	1.65
Salinity (psu)			
McCormick	2.19	6.18	7.53
Mud	−2.05	5.04	6.48
Trout	2.36	5.45	7.00
Taylor river	1.78	4.84	5.74
West highway	4.97	6.10	8.45

Errors are calculated relative to field data for daily average coastal creek discharges and coastal creek salinities. Mean errors were calculated by subtracting measured values from simulated values. Station locations are shown in Fig. 2. [ME, mean error; MAE, mean absolute error; RMSE, root mean square error; $m^3 s^{-1}$, cubic meters per second; m, meter; psu, practical salinity units].

with 5.43×10^8 m^3 for the base case), although volumetrically, this difference is less significant than for the five creeks with continuous data. Some minor differences between this simulation and the base case were noted for leakage rates, but in general the leakage pattern is similar to that for the base case (Fig. 8). These results, therefore, indicate that the upward leakage zone located midway between Old Ingraham Highway and the Buttonwood embankment (Fig. 8) is caused by topographic variations rather than by variable-density effects near the relatively dense saltwater wedge observed in the Biscayne aquifer.

The local wind stress was removed for the third simulation. A distinction is made here between local and regional wind effects. In SWIFT2D, the local wind stresses are included in the conservation of momentum equations (Eqs. (2) and (3)). The model allows input of temporally and/or spatially varying wind speed and direction for calculation of stress. On the other hand, regional wind effects are included in the limited domain model through specified water-level boundaries. For example, a strong southerly wind over Florida Bay will push water against the Buttonwood Embankment and raise water levels in northeastern Florida Bay. Thus, the water levels measured in northeastern Florida Bay, which are used to assign the southernmost stage boundary for the model, contain the effect of the regional wind field. Removing the local wind stress does not have a substantial effect on coastal creek flows, but does affect coastal salinities. As an example, observed and simulated (with and without local wind stress) daily average salinities at Trout Creek from November 2001 to July 2002 are shown in Fig. 10. Clearly, the simulation is improved when the local wind stress is included in the model, both in terms of the short-term fluctuations observed at the end of the 2001 wet season and in terms of the longer time increase in salinity as a result of the dry season.

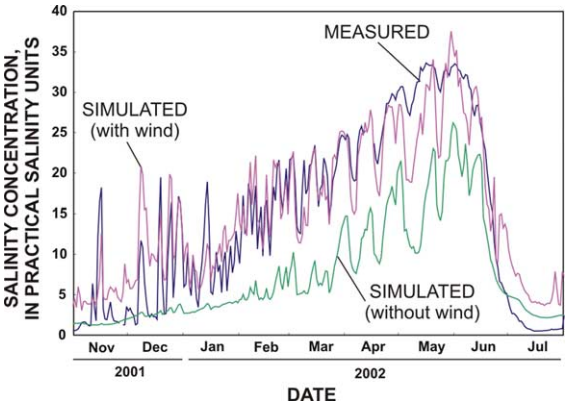

Fig. 10. Average daily salinity at Trout Creek from simulation without local wind stress, the base case simulation, and from measured data.

5. Discussion

Prior to performing simulations with the integrated model, the surface-water and ground-water models were independently developed and calibrated to the extent possible. For the initial surface-water model, exchange with ground water was considered negligible (Swain et al., 2004). Ground-water model development was performed after the surface-water model was developed, and thus simulated surface-water stages and salinities were applied as boundary conditions over the aquifer surface. This stepwise approach had two advantages. First, it was relatively easy to identify and correct input and runtime errors for the individual models before they were integrated. Second, computer runtimes for the ground-water

model were only a couple of hours, whereas the integrated model required over 30 h to run. The shorter computer runtimes were particularly useful during calibration of the ground-water model to aquifer salinity. Because of the highly transmissive nature of the Biscayne aquifer and a relatively stable freshwater/saltwater interface in southern Florida (Sonenshein, 1997), aquifer salinities were assumed to be in equilibrium with current water levels and hydrologic stresses. Thus, an additional level of confidence in the ground-water model was established when it could be shown that after the model reached dynamic equilibrium (through repeated simulations), the simulated freshwater/saltwater interface was in the observed location. Only minor salinity adjustments at the ground-water boundaries were required as part of this calibration process as hydrodynamic dispersion was not active for the simulations.

Limitations were periodically encountered using the explicit, time-lagged approach to couple the surface-water and ground-water models. For some sensitivity simulations with very large leakage rates, convergence could not be achieved during solution of the ground-water flow equation. Evaluation of the convergence problems indicated that very large leakage rates caused numerical oscillations in the implicit solution. Ground-water heads measured in the field can respond quickly to hydrologic stresses. For the Everglades application of the integrated model, however, large leakage rates may persist throughout the day in the model, because of the 1-day length of the stress period in SEAWAT, whereas actual leakage rates would decrease as ground-water heads respond more quickly. A decrease in the length of the ground-water stress period could probably have improved convergence. These convergence problems were encountered only in a few instances, and thus the day lag, which is computationally many times faster than using an hourly lag or fully implicit solution, was a necessity for this particular application. Future efforts using the integrated model should follow the example of Fairbanks et al. (2001) and focus on determining the relation between accuracy and efficiency for different coupling approaches and timestep lengths.

The Buttonwood Embankment clearly is an important physiographic feature in the Taylor Slough area. Model results and field observations suggest that freshwater flow into Florida Bay occurs primarily through the coastal creeks, rather than as overtopping of the embankment. This flow pattern has allowed field investigations to quantify with a high level of certainty the flow exchanges between the coastal wetlands and Florida Bay (Hittle, 2000; Hittle et al., 2001). Confidence in the predictive capability of the integrated model is due largely to the accuracy and long-term record length of creek discharge data. Many coastal wetlands in other locations, however, are not separated from the adjacent marine water body by an embankment or barrier to overland flow, and thus measurement of freshwater outflows is not as straightforward.

6. Summary and conclusions

This paper describes a numerical approach for simulating integrated surface-water/ground-water flow and solute transport in coastal wetlands and adjacent estuaries. The approach combines the SWIFT2D two-dimensional hydrodynamic flow and solute-transport code with the SEAWAT three-dimensional, saturated ground-water flow and solute-transport code. The surface-water and ground-water models, which both simulate density-dependent flow, are coupled using an explicit time-lagged approach based on a variable-density form of Darcy's Law to calculate the leakage flux at the ground surface; solute mass transfer between surface water and ground water is assumed to occur only by leakage advection.

The integrated code was applied to the southern Everglades of Florida and northeastern Florida Bay to quantify flow and salinity patterns for the period 1996–2002 and to evaluate the effects of selected hydrologic processes. In addition to simulating creek flows, the model also simulates overtopping of the coastal embankment and submarine ground-water discharge as mechanisms for delivering freshwater from the coastal wetlands into Florida Bay. Although simulated estimates of embankment overtopping contain a high level of uncertainty, model results indicate that overtopping is infrequent, but can occur in response to tropical storms. Storm surges force brackish Florida Bay water over the embankment and into the coastal wetlands. After making landfall,

a tropical storm can also produce enough rain to reverse embankment overflow from the coastal wetland into Florida Bay. The water budget for the coastal wetland part of the model domain indicates that average rates of downward leakage (17.42 cm yr^{-1}) and upward leakage (17.14 cm yr^{-1}) are nearly identical for the simulation period, but for any particular year, however, the wetland may experience a net loss or gain to or from the aquifer. Model results also indicate that submarine ground-water discharge may be occurring on the south side of the embankment in response to the higher surface-water levels in the coastal wetland.

Field data and model results indicate a strong seasonal pattern in coastal wetland salinities. Salinities at the coastal creeks reach 35 psu toward the end of the dry season, but quickly drop to less than 5 psu with the onset of the wet season. This seasonal flushing pattern is well represented by the model with MAEs in simulated salinity ranging between 4 and 7 psu for the five coastal creeks with continuous data for the 7-yr simulation period. Future modifications to the water-management system in southern Florida may alter the freshwater deliveries to the Taylor Slough area. Based on the performance of the model to match the seasonal flushing pattern, the model should be able to predict the effects of these altered water deliveries on coastal salinity patterns.

The effects of surface-water and ground-water interactions, density-dependent flow, and local wind stress were evaluated by performing simulations without these processes and comparing results with the base case simulation. In general, the surface-water model that neglects interactions with ground water compares worse with field data than the base case integrated model; however, without additional leakage measurements, the better match with the integrated model cannot be conclusively attributed to ground-water interactions. A constant-density simulation results in cumulative creek flows that are about 9% less than the base case, and only a slightly different pattern in leakage, suggesting that the upward leakage zone that coincides with the freshwater/saltwater interface in the Biscayne aquifer is caused by topographic variations rather than by density variations. Removing the local wind stress does not have a substantial effect on creek flows, but does affect coastal salinities. Without the local wind stress, Trout Creek salinities do not increase to the 30–35 psu values measured in the field during the dry season.

In general, comparisons between simulated and observed flow and salinity patterns in both the wetland and aquifer indicate that important system processes and behavior are represented by the model, and although the model is subject to limitations, it is well suited to predict the effects of Everglades restoration on the Taylor Slough coastal wetlands. The general approach described here would also be applicable to other coastal wetlands where restoration or contaminant transport issues are of concern. The integrated code is robust, accurate, and can represent hydrodynamic surface-water flow and variable-density ground-water flow for multi-year periods. Presently, the numerical tool is being used to evaluate the effects of the Comprehensive Everglades Restoration Plan on future hydrologic conditions (heads, flows, and salinities) in the coastal wetlands and adjacent Florida Bay estuary.

Acknowledgements

This study was funded by the US Geological Survey Priority Ecosystems Science Program and by the Everglades National Park Critical Ecosystem Studies Initiative. Development of the SEAWAT computer program was funded by the US Geological Survey Ground-Water Resources Program. The authors are grateful to John Wang, Mark Zucker, Eve Kuniansky, Weixing Guo, and an anonymous reviewer for providing substantial technical reviews of the manuscript. The authors would also like to acknowledge the contributions of Aaron Higer in recognizing the importance of coastal wetland hydrology and supporting the development of robust and accurate simulation tools.

References

Bakker, M., 2003. A Dupuit formulation for modeling seawater intrusion in regional aquifer systems. Water Resources Research 39 (5), 1131 doi: 10.1029/2002WR001710.

Bakker, M., Oude Essink, G.H.P., Langevin, C.D., 2004. The rotating movement of three immiscible fluids—a benchmark problem. Journal of Hydrology 287, 270–278.

Bales, J.D., Robbins, J.C., 1995. Simulation of hydrodynamics and solute transport in the Pamlico River Estuary, NC. US Geological Survey Open-File Report 94-454, 85pp.

Brown, G.L., McAdory, R.T., Nail, G.H., Sarruff, M.S., Berger, R.C., Granat, M.A., 2003. Development of a two-dimensional numerical model of hydrodynamics and salinity for Biscayne Bay, FL. US Army Corps of Engineers Technical Report CHL-03-10.

Desmond, G. 2003. Measuring and mapping the topography of the Florida Everglades for ecosystem restoration, in US Geological Survey Greater Everglades Science Program: 2002 Biennial Report April 13–18, 2003, US Geological Survey Open-File Report. 03-54, pp. 31–32

Fairbanks, J., Panday, S., Huyakorn, P.S., 2001. Comparisons of linked and fully coupled approaches to simulating conjunctive surface/subsurface flow and their interactions. In: Seo, B., Poeter, E., Zheng, C. (Eds.), MODFLOW 2001 and Other Modeling Odysseys, Conference Proceedings, Golden, CO, pp. 356–361.

Fischer, H.B., List, J.E., Koh, R.C.Y., et al., 1979. Mixing in Inland and Coastal Waters, 263. Academic Press, New York (pp. 126–127).

Fitterman, D.V., Deszcz-Pan, M., 1998. Helicopter EM mapping of saltwater intrusion in Everglades National Park. Florida Exploration Geophysics 29, 240–243.

Fitterman, D.V., Deszcz-Pan, M., Stoddard, C.E., 1999. Results of time-domain electromagnetic soundings in Everglades National Park, FL. US Geological. Survey Open-File Report 99-426

Fish, J.E., Stewart, M.T., 1991. Hydrogeology of the surficial aquifer system, Dade County, FL. US Geological Survey Water Resources Investigations Report. 90-4108, 50pp.

German, E.R., 1999. Regional evaluation of evapotranspiration in the Everglades, in Proceedings of the Third International Symposium on Ecohydraulics, Salt Lake City, UT, July 13–16.

German, E.R., 2000a. Regional evaluation of evapotranspiration in the Everglades. US Geological Survey Water-Resources Investigations Report 00-4217, 48pp.

German, E.R., 2000b. Regional evaluation of evapotranspiration in the Everglades. In: Eggleston et al. (Ed.), US Geological Survey Program on the South Florida Ecosystem: 2000 Proceedings of the Greater Everglades Ecosystem Restoration (GEER) Conference, December 11–15, 2000 US Geological Survey Open-File Report 00-449, pp. 21–23.

Goodwin, C.R., 1987. Tidal-flow, circulation, and flushing changes caused by dredge and fill in Tampa Bay, Florida. US Geological Survey Water-Supply Paper 2282. 88pp..

Goodwin, C.R., 1991. Tidal-flow, circulation, and flushing changes caused by dredge and fill in Hillsborough Bay, Florida. US Geological Survey Water-Supply Paper 2376. 49pp..

Goodwin, C.R., 1996. Simulation of tidal-flow, circulation, and flushing of the Charlotte Harbor Estuarine System, FL. US Geological Survey Water-Resources Investigations Report 93-4153, 92pp.

Graham, D.N., Refsgaard, A., 2001. MIKE SHE: a distributed, physically based modeling system for surface water/groundwater interactions. In: Seo, B., Poeter, E., Zheng, C. (Eds.), MODFLOW 2001 and Other Modeling Odysseys, Conference Proceedings, Golden, CO, pp. 321–327.

Guo, W., Bennett, G.D., 1998. Simulation of saline/fresh water flows using MODFLOW, in MODFLOW 98 Conference, Golden, CO. In: Poeter, E. et al. (Ed.), 1998 Proceedings (1), pp. 267–274.

Guo, W., Langevin, C.D., 2002. User's guide to SEAWAT: a computer program for simulation of three-dimensional variable-density ground-water flow: US Geological Survey Open-File Report 01-434, 79pp.

Hansen, M., DeWitt, N.T., 2000. 1890 and 1990 bathymetry of Florida Bay. US Geological Survey Open-File Report 00-347. http://sofia.usgs.gov/publications/ofr/00-347/.

Harvey, J.W., Choi, J., Mooney, R.H., 2000a. Hydrologic interactions between surface water and ground water in Taylor Slough, Everglades National Park. In: Eggleston et al. (Ed.), US Geological Survey Program on the South Florida Ecosystem: 2000 Proceedings of the Greater Everglades Ecosystem Restoration (GEER) Conference, December 11–15, 2000 US Geological Survey Open-File Report 00-449, pp. 24–26.

Harvey, J.W., Jackson, J.M., Mooney, R.H., Choi, J., 2000b. Interactions between ground water and surface water in Taylor Slough and Vicinity, Everglades National Park, south Florida: Study Methods and Appendixes. US Geological Survey Open-File Report 00-483, 67pp.

Hittle, C.D., 2000. Quantity, timing, and distribution of freshwater flows into northeastern Florida Bay. In: Eggleston et al. (Ed.), US Geological Survey Program on the South Florida Ecosystem: 2000 Proceedings of the Greater Everglades Ecosystem Restoration (GEER) Conference, December 11–15, 2000 US Geological Survey Open-File Report 00-449, pp. 27–28.

Hittle, C.D., Patino, E., Zucker, M.A., 2001. Freshwater flow from estuarine creeks into northeastern Florida Bay. US Geological Survey Water-Resources Investigations Report 01-4164, 32pp.

Holmes, C.W., Robbins, J., Halley, R., Bothner, M., Ten Brink, M., Marot, M., 2000. Sediment dynamics of Florida Bay mud banks on a decadal time scale. In: Eggleston et al. (Ed.), US Geological Survey Program on the South Florida Ecosystem: 2000 Proceedings of the Greater Everglades Ecosystem Restoration (GEER) Conference, December 11–15, 2000 US Geological Survey Open-File Report 00-449, p. 108.

HydroGeoLogic Inc., 2003. MODHMS—a comprehensive MODFLOW-based hydrologic modeling system, Version 2.1, HydroGeoLogic Inc., Herndon, VA.

Jarosewich, M., Wagner, J., 1985. Geologic structure of the surficial aquifer system underlying Everglades National Park and the Big Cypress National Preserve, 43pp, Everglades National Park, South Florida Research Center, Homestead, FL.

Jenter, H.L., Duff, M.P., 1999. Locally-forced wind effects on shallow waters with emergent vegetation, in Proceedings of the 3rd International Symposium on Ecohydraulics, Salt Lake City, UT, July 13–16.

Juster, T.C., 1995. Circulation of saline and hypersaline groundwater in carbonate mud: mechanisms, rates, and an example from Florida Bay. PhD Dissertation, University of South Florida, Tampa, FL, 215pp.

Kohout, F.A., 1964. The flow of fresh water and salt water in the Biscayne aquifer of the Miami area, Florida, in Sea Water in Coastal Aquifers. US Geological Survey Water-Supply Paper 1613-C, pp. 12–32.

Knight, E.L., Kotun, K., James, F.E., 2000. An evaluation of the hydrologic conditions resulting from Hurricane Irene in Everglades National Park, DRAFT, 94pp. South Florida Natural Resources Center, Everglades National Park, Homestead, FL.

Langevin, C.D., 2001. Simulation of ground-water discharge to Biscayne Bay, Southeastern Florida. US Geological Survey Water-Resources Investigations Report 00-4251, 127pp.

Langevin, C.D., 2003. Simulation of submarine ground water discharge to a marine estuary: Biscayne Bay Florida. Ground Water 41 (6), 758–771.

Langevin, C.D., Shoemaker, W.B., Guo, W., 2003. MODFLOW-2000, the US Geological Survey modular ground-water model-documentation of the SEAWAT-2000 version with the variable-density flow process (VDF) and the integrated MT3DMS transport process (IMT), US Geological Survey Open-File Report 03-426, 43pp.

Langevin, C.D., Swain, E.D., Wolfert, M.A., 2004. Simulation of integrated surface-water/fround-water flow and salinity for a coastal wetland and adjacent estuary: US Geological Survey Open-File Report 2004-1097.

Large, W.G., Pond, S., 1981. Open ocean momentum flux measurements in moderate to strong winds. Journal of Physical Oceanography 11, 324–336.

Lee, J.K., Carter, V., Rybicki, N.B., 1999. Determining flow-resistance coefficients in the Florida Everglades, in Proceedings of the Third International Symposium on Ecohydraulics, Salt Lake City, UT, July 13–16.

Lee, J.K., Jenter, H.L., Lai, V.C., Visser, H.M., Duff, M.P., 2000. A pipe manometer for the determination of very small water-surface slopes in the Florida Everglades. In: Eggleston et al. (Ed.), US Geological Survey Program on the South Florida Ecosystem: 2000 Proceedings of the Greater Everglades Ecosystem Restoration (GEER) Conference, December 11–15, 2000 US Geological Survey Open-File Report 00-449, pp. 31–32.

Leendertse, J.J., 1972. A Water-quality simulation model for well-mixed estuaries and coastal seas: Volume IV, Jamaica Bay tidal flows, NY, 48pp., The New York City Rand Institute, R-1009-NYC.

Leendertse, J.J., 1987. Aspects of SIMSYS2D, a system for two-dimensional flow computation. Santa Monica, CA, Rand Corporation Report R-3572-USGS, 80pp.

Leendertse, J.J., Gritton, E.C., 1971. A water-quality simulation model for well-mixed estuaries and coastal seas: Volume II, Computation procedures: 48pp. New York, The New York City Rand Institute, R-708-NYC.

Leendertse, J.J., Langerak, A., de Ras, M.A.M., 1981. In: Fischer, H.B. (Ed.), Two-dimensional tidal models for the delta works Transport models for inland and coastal waters, Proceedings of a Symposium on Predictive Ability. Academic Press, New York.

Lusczynski, N.J., 1961. Head and flow of ground water of variable density. Journal of Geophysical Research 66, 4247–4256.

McDonald, M.G., Harbaugh, A.W., 1988. A modular three-dimensional finite-difference ground-water flow model. US Geological Survey Techniques of Water-Resources Investigations, Book 6, Chapter A1, 586pp.

McDonald, M.G., Harbaugh, A.W., Orr, B.R., Ackerman, D.J., 1992. A method of converting no-flow cells to variable-head cells for the US Geological Survey modular finite-difference ground-water flow model. US Geological Survey Open-File Report 91-536, 99pp.

Merritt, M.L., 1996a. Simulation of the water table altitude in the Biscayne aquifer, southern Dade County, FL, water years 1945–1989. US Geological Survey Water-Supply Paper 2458, 148pp.

Merritt, M.L., 1996b. Numerical simulation of a plume of brackish water in the Biscayne aquifer originating from a flowing artesian well, Dade County, FL. US Geological Survey Water-Supply Paper 2464, 74pp.

Nuttle, W.K., Forqurean, J.W., Cosby, B.J., Zieman, J.C., Robblee, M.B., 2000. Influence of net freshwater supply on salinity in Florida Bay. Water Resources Research 36 (7), 1805–1822.

Panday, S., Huyakorn, P.S., 2004. A fully coupled physically-based spatially-distributed model for evaluating surface/subsurface flow. Advances in Water Resources 27(4), 361–382.

Prager, E., Halley, R., 1997. Florida Bay bottom types. US Geological Survey Open-File Report 97-526, 1pp.

Price, R.M., 2001. Geochemical determinations of groundwater flow in Everglades National Park, PhD Dissertation, University of Miami, Coral Gables, FL, 235pp.

Reid, R.O., Whitaker, R.E., 1976. Wind-driven flow of water influenced by a canopy. Journal of the Waterways, Harbors, and Coastal Engineering Division 102 (WW1), 61–77.

Robbins, J.C., Bales, J.D., 1995. Simulation of hydrodynamics and solute transport in the Neuse River Estuary, NC. US Geological Survey Open-File Report 94-511, 85pp.

Sonenshein, R.S., 1997. Delineation and extent of saltwater intrusion in the Biscayne aquifer, Eastern Dade County, FL, 1995. US Geological Survey Water-Resources Investigations Report 96-4285, 1 sheet.

Stewart, M.A., Bhatt, T.N., Fennema, R.J., Fitterman, D.V., 2002. The road to Flamingo: an evaluation of flow pattern alterations and salinity intrusion in the lower glades, Everglades National Park. US Geological Survey Open-File Report 02-59, 36pp.

Swain, E.D., Howie, B., Dixon, J., 1996. Description and field analysis of a coupled ground-water/surface-water flow model (MODFLOW/BRANCH) with modifications for structures and wetlands in southern Dade County, FL. US Geological Survey Water-Resources Investigations Report 96-4118, 67pp.

Swain, E.D., Wolfert, M., Bales, J.D., Goodwin, C.R., 2004. Two-dimensional hydrodynamic simulation of surface-water flow and transport to Florida Bay through the Southern Inland and Coastal Systems (SICS). US Geological Survey Water-Resources Investigations Report 03-4287, 56pp.

Tillis, G.M., 2001. Measuring Taylor slough boundary and internal flows, Everglades National Park, FL. US Geological Survey Open-File Report 01-225, 16pp.

VanderKwaak, J.E., 1999. Numerical simulation of flow and chemical transport in integrated surface-subsurface hydrologic systems, PhD Dissertation, Department of Earth Sciences, University of Waterloo, Ont., Canada, 217pp.

VanderKwaak, J.E., Loague, K., 2001. Hydrologic-response simulations for the R-5 catchment with a comprehensive physics-based model. Water Resources Research 37 (4), 999–1013.

Wang, J.D., Luo, J., Ault, J.S., 2003. Flows, salinity, and some implications for larval transport in South Biscayne Bay, FL. Bulletin of Marine Science 73 (3), 695–723.

Yeh, G.T., Huang, G.B., 2003. A numerical model to simulate water flow in watershed systems of 1-D stream-river network, 2-D overland regime, and 3-D subsurface media (WASH123D: Version 1.5), Technical Report. Department of Civil and Environmental Engineering, University of Central Florida, Orlando, FL.

Zheng, C., Wang, P.P., 1999. MT3DMS—a modular three-dimensional multispecies transport model for simulation of advection, dispersion and chemical reactions of contaminants in ground-water systems; documentation and user's guide, US Army Corps of Engineers Contract Report SERDP-99-1.